Why Are Alkali Halide Surfaces Not Wetted by Their Own Melt?

T. Zykova-Timan,[1] D. Ceresoli,[1] U. Tartaglino,[1,2] and E. Tosatti[1,3]

[1]*International School for Advanced Studies (SISSA) and INFM Democritos National Simulation Center, Via Beirut 2-4, I-34014 Trieste, Italy*

[2]*IFF, FZ-Jülich, 52425 Jülich, Germany*

[3]*International Centre for Theoretical Physics (ICTP), P.O. Box 586, I-34014 Trieste, Italy*

(Received 5 November 2004; revised manuscript received 9 February 2005; published 5 May 2005)

Alkali halide (100) crystal surfaces are anomalous, being very poorly wetted by their own melt at the triple point. We present extensive simulations for NaCl, followed by calculations of the solid-vapor, solid-liquid, and liquid-vapor free energies showing that solid NaCl(100) is a nonmelting surface, and that its full behavior can quantitatively be accounted for within a simple Born-Meyer-Huggins-Fumi-Tosi model potential. The incomplete wetting is traced to the conspiracy of three factors: surface anharmonicities stabilizing the solid surface; a large density jump causing bad liquid-solid adhesion; incipient NaCl molecular correlations destabilizing the liquid surface. The latter is pursued in detail, and it is shown that surface short-range charge order acts to raise the surface tension because incipient NaCl molecular formation anomalously reduces the surface entropy of liquid NaCl much below that of solid NaCl(100).

DOI: 10.1103/PhysRevLett.94.176105 PACS numbers: 68.03.Cd, 68.08.Bc, 68.08.De

Molten alkali halides and their surfaces have long been studied experimentally [1,2] and theoretically [2–7]. Much less attention has been devoted to solid alkali halide surfaces at high temperatures, and especially to their wetting habit at the melting point. Yet, these crystal surfaces behave anomalously in that respect. Whereas most liquids would wet their own solid-vapor interfaces—the solid surfaces undergoing surface melting at the melting point T_m (triple point wetting [8])—molten salts wet their own solid surface only incompletely. The external and internal contact angles θ and ϕ of a partially wetting liquid droplet onto its own solid are connected to the free energies γ of the solid-vapor (SV), solid-liquid (SL), and liquid-vapor (LV) interfaces by Young's equation [9]:

$$\gamma_{\mathrm{SV}} = \gamma_{\mathrm{SL}} \cos\phi + \gamma_{\mathrm{LV}} \cos\theta. \quad (1)$$

Incomplete, or partial, triple point wetting, with $\phi \sim 0$ but with $\theta > 0$ and stable near T_m, implies that some physical mechanism must be at work making $\gamma_{\mathrm{SV}} < \gamma_{\mathrm{SL}} + \gamma_{\mathrm{LV}}$. For liquid NaCl on NaCl(100) at $T_m = 1074$ K, a partial wetting angle $\theta \sim 48°$ is well established, with similar results holding for other alkali halides too [10,11]. This angle is exceptionally large—and thus the corresponding self-wetting at the triple point is exceptionally poor—even when compared with strongly nonwetting metal surfaces, where, e.g., $\theta \sim 15°$ measured for liquid Pb/Pb(111) [12] or $\sim 18°$ obtained by a simulation of liquid Al/Al(111) [13]. Should liquid surface layering [14] be, as in the case of metals [13,15], the culprit for the incomplete wetting of alkali halides too, the layering magnitude and its effects should be exceptionally strong. However, all of the existing molten salt theory and simulations indicate the opposite, namely, a soft, smooth, layering-free liquid-vapor interface [5–7]. This leaves partial wetting wide open for another explanation. In a more general context, it seems desirable to pursue a case study of solid-liquid-vapor coexistence at the triple point in a simple but realistic model that could be addressed at the fully microscopic level. We wish, in particular, to understand what may control wetting and adhesion in a specific and chemically unambiguous case such as that of a liquid with its own solid. For these reasons, and in order to shed light on the underlying physics, we undertook extensive simulations of the NaCl(100) solid surface, of the liquid NaCl surface, and of the solid-liquid interface around T_m.

NaCl, our prototype alkali halide, was described by the classic Born-Mayer-Huggins-Fumi-Tosi (BMHFT) two-body potential [16]. Polarization forces, though not negligible [6], were sacrificed in the present context, where computational simplicity is essential to reach a unified description of all possible interfaces with very large sizes and simulation times. Eventually, as it turns out, quantitative accuracy in the description of NaCl interfaces seems anyway quite good in the BMHFT model.

Bulk systems were first simulated by molecular dynamics (MD) at constant volume with cubic simulation cells comprising up to about 5000 NaCl units. Surfaces were studied with periodically repeated slabs, consisting of 12–24 planes with 64 NaCl units each, separated by 100–120 Å of vacuum. We treated long-range forces in full using a 3D Ewald summation. Despite the size and time limitations imposed by long-range forces, great care was taken to run simulations long enough for a clear equilibration, typically 100–300 ps at T_m. In preliminary bulk simulations, we determined the equilibrium lattice spacing $a(T)$ as a function of temperature at zero pressure. All subsequent simulations were then performed at fixed cell size, by enforcing $a(T)$ at each temperature. The calculated room temperature $a(T_R)$ and linear expansion coefficient, 5.683 Å and 40.5×10^{-6} K^{-1}, are in very good

agreement with experiment, 5.635 Å and 38.3×10^{-6} K^{-1}. The bulk melting temperature T_m (practically identical to the triple point temperature owing to Clapeyron's equation) was established by simulation of liquid-solid coexistence at zero pressure and was found to be 1066 ± 20 K (1074 K experimental) [17]. This value is also in perfect agreement with 1064 ± 14 K, independently obtained for the BMHFT potential by Anwar *et al.* [20]. Our theoretical volume expansion and latent heat of melting are 27% and 0.2899 (experimental 26% and 0.2915 eV/molecule [1]). Full details will be presented in a forthcoming paper [19].

In surface MD simulations, defect-free NaCl(100) was first of all found to remain indefinitely solid and totally dry for all temperatures up to T_m, and for even the longest simulation times ~1 ns. Moreover, in a metastable state, simulated NaCl(100) remained crystalline even above T_m. By melting initially a few surface layers, and then observing in a subsequent canonical MD run that these liquid layers spontaneously recrystallized even above T_m [21], we established the existence of a multimonolayer thick nucleation barrier against surface melting up to about 1115 K $\simeq T_m + 50$ K, then a thin monoatomic nucleation barrier until 1215 K $\simeq T_s = T_m + 150$ K. Only at T_s, well above T_m, does solid NaCl(100) become locally unstable and spontaneously melt. This metastable behavior was found to persist even in the presence of surface defects, such as molecular vacancies [22] or steps, at least up to 1115 K [19]. Altogether, these results characterize NaCl(100) as a clear case of surface nonmelting [12,15,21], a prediction that deserves to be tested in experiment. For a short enough time, it should be possible, for example, to overheat NaCl(100) and other alkali halide surfaces substantially above T_m without melting them.

Next, we proceeded to simulate the liquid NaCl surface, more precisely melted NaCl slabs. The (x, y) averaged liquid local density profile $\rho(z)$ [Fig. 1(d)] is confirmed to be remarkably smooth as found in previous studies [5–7], devoid of layering unlike Al, Pb [Figs. 1(a) and 1(b)], and much more diffuse [Fig. 1(d)] than even that of liquid Ar [Fig. 1(c)].

The nature of diffuseness of the NaCl surface is demonstrated by the simulation snapshot of Fig. 2(a), showing very pronounced fluctuations [23], in the instantaneous surface profile. This picture is suggestive of a low surface tension, high entropy surface, in apparent contradiction with the massive nonwetting of solid NaCl(100) by its melt, which is favored only by a sufficiently large γ_{LV} [Eq. (1)].

In order to clarify the situation, we undertook direct calculations of interface free energies γ_{SV}, γ_{LV}, and γ_{SL}. We obtained γ_{LV} as the surface stress of the simulated liquid slab (two interfaces) through the Kirkwood-Buff formula:

$$\begin{aligned}\gamma_{LV} &= \frac{1}{2}\int_0^{L_z} dZ[\sigma_{\parallel}(Z) - \sigma_{\perp}(Z)] \\ &= -\frac{1}{8}\sum_{\alpha,\beta}\int_{-\infty}^{\infty} dZ \int d^3\mathbf{r}_{ij}\frac{x_{ij}^2 + y_{ij}^2 - 2z_{ij}^2}{r_{ij}} \\ &\quad \times[\delta_{\alpha\beta} + \lambda(1-\delta_{\alpha\beta})] f_{\alpha\beta}(r_{ij}) g_{\alpha\beta}(\mathbf{r}_{ij}; Z)\rho_{\alpha}(Z)\rho_{\beta}(Z) \\ &= -\frac{1}{8L_xL_y}\left\langle \sum_{i,j}\frac{x_{ij}^2 + y_{ij}^2 - 2z_{ij}^2}{r_{ij}} \right. \\ &\quad \left. \times[\delta_{\alpha\beta} + \lambda(1-\delta_{\alpha\beta})] f_{\alpha\beta}(r_{ij}) \right\rangle, \end{aligned} \tag{2}$$

where $(\alpha, \beta) = (+, -)$, Z is the distance normal to the interface, L_x, L_y are the supercell sizes, and $\sigma_{\parallel} = \frac{1}{2}(\sigma_{xx} + \sigma_{yy})$ and $\sigma_{\perp} = \sigma_{zz}$ are normal and tangential components of the stress tensor, respectively. Here $\langle \cdots \rangle$ denotes a canonical average, $\sum_{i,j}$ is over all pairs of particles, $\mathbf{r}_{ij}$ is the distance between atoms i and j, $f_{\alpha\beta}(r_{ij})$ is the force between them, $g_{\alpha\beta}(\mathbf{r}_{ij}; Z)$ are the Na-Cl (Na-Na, Cl-Cl) pair correlation functions measured in a slice centered at Z, $\rho_{\alpha}(Z)$ is the average density of an ion α near Z, and λ is a parameter here equal to one, inserted for later use. As

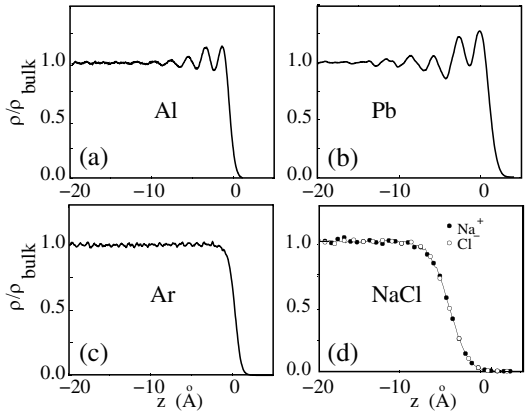

FIG. 1. Simulated density profile of liquid surfaces [15] of (a) Al, (b) Pb, (c) LJ (Ar) in comparison with (d) ρ(Na) and ρ(Cl) profiles in NaCl at T_m; solid line, average of the two.

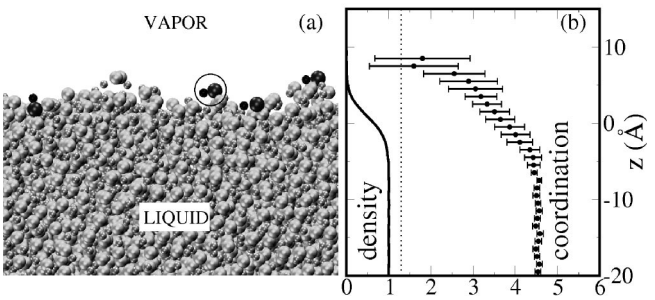

FIG. 2. (a) Simulation snapshot of the NaCl liquid surface at T_m. Notice the large thermal fluctuations and some nearly molecular configurations highlighted in the outermost region. (b) Coordination number $N(Z)$ and the density profile showing the smooth crossover from liquid ($N = 4.6$) to molecular vapor ($N = 1.3$, dotted line). Density profile as in Fig. 1 in units ρ/ρ_{bulk}.

shown in Fig. 3(b), γ_{LV} so obtained compares well against experiment [1], for example, at T_m, $\gamma_{LV} = 104 \pm 8$ mJ/m^2 against 116 mJ/m^2.

The free energy γ_{SV} of solid NaCl(100) was obtained by thermodynamic integration $\gamma_{SV}/T = \gamma_{SV,0}/T_0 + \int_{T_0}^{T} d(1/T')\Delta E(T')$, where $\Delta E(T)$ is the surface excess internal energy obtained by simulation, and $T_0 = 50$ K was chosen as a convenient reference state (our simulations are classical and do not include quantum freezing). The results of Fig. 3(a) show a relatively low γ_{SV}, characterized by a drop from 210 mJ/m^2 at 50 K to $\sim$100 mJ/m^2 at T_m. The drop confirms that the exceptional stability of solid NaCl(100) is significantly enhanced by anharmonicity above 600 K. To gauge the nature of anharmonicity, we extracted from velocity-velocity correlations the T-dependent frequency spectrum of a slab and of a bulk sample with the same number of molecular units. Treating both spectra as collections of harmonic oscillators, two harmonic free energies can be calculated. Half their difference yields an effective harmonic γ_{SV}^{harm}, whose milder drop with temperature, due to surface vibrational softening, is seen to recover about half the true solid surface entropy $S_{SV} = -d\gamma_{SV}/dT$. The remaining half thus represents an additional stabilization of the solid surface by ''hard'' anharmonicity.

Finally, γ_{SL} in the BMHFT model was calculated by inserting in Eq. (1) the calculated γ_{SV}, γ_{LV}, and the contact angles $\theta = 50° \pm 5°$, $\phi \sim 0°$, obtained by separate simulation of a liquid droplet deposited on NaCl(100) [24]. We obtained $\gamma_{SL} = 36 \pm 6$ mJ/m^2 in this manner. A charged hard sphere [7] study along the lines proposed, e.g., for neutral hard spheres [18] might be desirable in order to rationalize this result. Our relatively large γ_{SL} indicates poor adhesion of the liquid to the solid substrate, attributable to the unusually large difference of density and structure between liquid and solid [17].

While the result $\gamma_{SV} \simeq \gamma_{SL} + \gamma_{LV} - 40$ mJ/m^2 now fully accounts for the nonmelting of NaCl(100) and its incomplete triple point wetting, it does not yet clarify the role of the liquid NaCl surface in this context. This can be addressed in more depth by considering the calculated

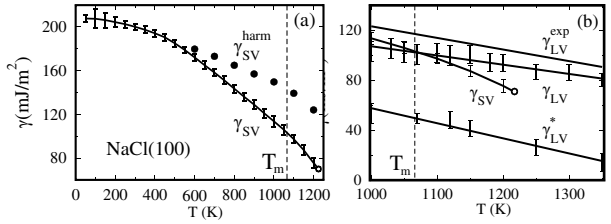

FIG. 3. Calculated NaCl surface free energies. (a) Solid-vapor γ_{SV}. Note the metastability up to about 150 K above T_m. Dots, effective harmonic approximation. (b) Liquid-vapor γ_{LV}. Experimental data from Ref. [1] and references therein. γ^*_{LV}, hypothetical liquid surface free energy calculated by setting $\lambda = 0$ for outer surface atoms with coordination below 1.3 [highlighted in Fig. 2(a)].

temperature dependence of the surface tension γ_{LV} (Fig. 3). Strikingly, the temperature dependent drop of surface free energy shows a factor 2.6 *lower* surface entropy $S_{LV} = -d\gamma_{LV}/dT$ of the liquid surface compared with that S_{SV} of the solid surface. This is contrary to naive expectations, based on the picture of a relatively ordered, defect-free solid surface and a very disordered, strongly fluctuating liquid surface. The presence of this ''liquid surface entropy deficit'' (SED) suggests some underlying short-range order, which could also explain why the liquid surface tension here is surprisingly as high as that of the solid surface. The surface order, if any, is clearly not layering: so what could it be instead?

The answer, as was foreshadowed earlier on [3], is that charge order, already important in bulk, plays an enhanced role at the molecular liquid surface. If surface thermal fluctuations are indeed large, we find them revealingly *correlated*. For a Na^+ ion that instantaneously moves, e.g., out of the surface, there is at least one accompanying Cl^- also moving out, and vice versa. So while large surface fluctuations smear the overall liquid-vapor density profile bridging gently between the liquid and the vapor [Fig. 1(d)], the two-body correlations, described, e.g., by the Na-Cl pair correlation function $g_{+-}(\mathbf{r})$, or by its integral, the ion coordination number N, drop from values typical of the bulk liquid at T_m to the nonzero value of the molecular vapor, instead of zero as in the Lennard-Jones (LJ) liquid. For a more quantitative understanding, we calculated a locally defined charge coordination number:

$$N(Z) = \frac{1}{2\zeta} \int_{Z-\zeta}^{Z+\zeta} dZ' \rho(Z') \int_{r<r_m} d^3\mathbf{r} g_{+-}(r; Z'), \qquad (3)$$

where $r_m = 4$ Å corresponds to the first local minimum of $g_{+-}(r)$, and ζ is a small interval. Starting with the ideal $N_S = 6$ of the solid, we have $N_L = 4.6$ in the bulk liquid at T_m. Moving across the liquid-vapor interface, $N(Z)$ drops continuously from 4.6 downward [Fig. 2(b)]. Even if simulation statistics is lost, $N(Z)$ remains for large Z larger than or equal to $N_V \simeq 1.3$, the value appropriate for NaCl vapor (which at T_m consists for 69% of NaCl molecules, and 31% of dimers [25]). The larger the coordination number of atoms in the interface region, the less their configurational entropy and the higher the surface tension. Hence incipient molecular order could be the reason for the SED of liquid NaCl.

For a test of this idea, we repeated the surface tension calculation of liquid NaCl by only slightly and artificially altering in Eq. (2) the value of correlations g_{+-} or, which is equivalent, of the forces acting among Na and Cl for the (extremely small) fraction of outermost surface atoms whose coordination number $N \lesssim 1.3$. Since the dynamics, and thus the internal energy, remain untouched in this way, the contribution of these configurations to the surface stress gives a direct measure of the negative surface entropy contribution to the surface tension caused by molecular

short-range order at the liquid-vapor interface. We first identified in simulations the surface Na and Cl ions by means of a simple algorithm. We then extracted their mean electrostatic potential value V_i, and established a roughly linear connection between atom potential and coordination [19,26]. Finally, we modified the Coulomb part of the charge contribution in Eq. (2) of surface Na^+ ions in the form $\lambda = \Theta(V_0 - V_i)$, where Θ is the step function and $V_0 = -6.99$ eV is the value that cancels correlations for Na^+ ions with $N \leq 1.3$. Though representing an exceedingly small fraction of the surface atoms [Fig. 2(a)], removal of the surface stress contribution by these molecularly paired Na and Cl ions yields a considerable surface tension drop from $\gamma_{LV} = 104$ mJ/m^2 to $\gamma^*_{LV} = 53$ mJ/m^2 (Fig. 3). The increased temperature slope $|d\gamma^*_{LV}/dT|$ exactly matches the calculated drop from γ_{LV} to γ^*_{LV}, confirming that it corresponds to a purely entropic gain—the removal of some of the SED through the cancellation of molecular surface correlations. Since now $\gamma^*_{LV} + \gamma_{SL} < \gamma_{SV}$ (the equivalent correction to γ_{SL} and γ_{SV} is utterly negligible), recovery of this surface entropy actually suffices to provoke *complete* instead of partial wetting of NaCl(100) at the melting point.

In conclusion, we found that BMHFT potential simulations and the related surface thermodynamics explain quantitatively the incomplete wetting of NaCl(100) by liquid NaCl at the triple point. Three elements, namely, the exceptional anharmonic stability of the solid (100) surface, the poor adhesion of the liquid onto the solid, and a liquid surface entropy deficit caused by incipient molecular short-range charge order, all conspire to give rise to this phenomenon in the BMHFT model of NaCl, and most likely also in real alkali halide surfaces.

Experimentally, it should be possible to demonstrate the overheating of NaCl(100) and other alkali halide surfaces, perhaps in the same way as in metals [27] (though here the high vapor pressure at T_m suggests using techniques not relying on ultrahigh vacuum). The poor adhesion of the molten salt onto its own solid should be detectable in nucleation. The short-range correlations described at the surface of molten salts could possibly become accessible spectroscopically. Also, if these surface correlations could, for example, be altered by external means, e.g., by electric fields, the wetting angle should change accordingly. Finally, the general possibility that some form of short-range order at the liquid-vapor interface might affect the surface tension by reducing surface entropy could be of wider relevance to other compound and molecular liquid surfaces.

This work was sponsored by MIUR FIRB RBAU017S8 R004, FIRB RBAU01LX5H, and MIUR COFIN 2003 and 2004, as well as by INFM (Iniziativa trasversale calcolo parallelo). We acknowledge illuminating discussions with E. A. Jagla and A. C. Levi, and the early collaboration of W. Sekkal.

[1] G. Janz, *Molten Salts Handbook* (Academic Press, New York, 1967).
[2] C. A. Croxton, *Statistical Mechanics of the Liquid Surface* (J. Wiley, Chichester, 1980).
[3] R. W. Pastor and J. Goodisman, J. Chem. Phys. **68**, 3654 (1978).
[4] R. Evans and T. J. Sluckin, Mol. Phys. **40**, 413 (1980).
[5] D. M. Heyes, Phys. Rev. B **30**, 2182 (1984).
[6] A. Aguado, M. Wilson, and P. A. Madden, J. Chem. Phys. **115**, 8603 (2001); A. Aguado, W. Scott, and P. A. Madden, J. Chem. Phys. **115**, 8612 (2001).
[7] B. Groh, R. Evans, and S. Dietrich, Phys. Rev. E **57**, 6944 (1998); M. González-Melchor, J. Alejandre, and F. Bresme, Phys. Rev. Lett. **90**, 135506 (2003).
[8] See, e.g., S. Dietrich, in *Phase Transitions and Critical Phenomena*, edited by C. Domb and J. Lebowitz (Academic Press, London, 1988), Vol. 12, p. 1.
[9] P. Nozières, J. Phys. (France) **50**, 2541 (1989).
[10] G. Grange and B. Mutaftschiev, Surf. Sci. **47**, 723 (1975).
[11] L. Komunjer *et al.*, J. Cryst. Growth **182**, 205 (1997).
[12] B. Pluis *et al.*, Phys. Rev. Lett. **59**, 2678 (1987).
[13] F. D. Di Tolla *et al.*, Phys. Rev. Lett. **74**, 3201 (1995).
[14] H. L. Lemberg, S. A. Rice, and D. Guidotti, Phys. Rev. B **10**, 4079 (1974).
[15] U. Tartaglino, T. Zykova-Timan, F. Ercolessi, and E. Tosatti, Phys. Rep. (to be published).
[16] F. G. Fumi and M. P. Tosi, J. Phys. Chem. Solids **25**, 31 (1964).
[17] Simulation snapshots also showed an exceptionally sharp solid-liquid interface [18,19], suggesting a large γ_{SL}, later confirmed.
[18] B. B. Laird, J. Chem. Phys. **115**, 2887 (2001).
[19] T. Zykova-Timan, U. Tartaglino, D. Ceresoli, and E. Tosatti (to be published).
[20] J. Anwar, D. Frenkel, and M. G. Noro, J. Chem. Phys. **118**, 728 (2003).
[21] P. Carnevali, F. Ercolessi, and E. Tosatti, Phys. Rev. B **36**, 6701 (1987).
[22] Evaporation of molecules and molecular dimers, an event too rare to take place efficiently in simulations, does not appreciably alter the solid surface behavior described, which applies to the large flat solid terraces in sublimation equilibrium with the vapor at and above T_m. Similarly, in liquid surface simulations the vapor is essentially absent, but the properties derived should be indistinguishable from those of the fully equilibrated liquid-vapor interface.
[23] Capillary wave induced smearing of the profile was checked and found to be practically irrelevant at our small sizes [19]. See, however, Ref. [6].
[24] T. Zykova-Timan *et al.*, Surf. Sci. **566–568**, 794 (2004).
[25] P. Davidovits and D. L. McFadden, *Alkali Halide Vapors: Structure, Spectra, and Reaction Dynamics* (Academic Press, New York, 1979).
[26] The value of $-V_0$ at Na is 6.80 eV in the NaCl simulated molecule, 7.485 eV in Na_2Cl_2, 7.82 eV in Na_3Cl_3, 8.32 eV for liquid NaCl, and 8.57 eV for solid NaCl both at T_m.
[27] J. W. Herman and H. E. Elsayed-Ali, Phys. Rev. B **49**, 4886 (1994); J. J. Métois and J. C. Heyraud, J. Phys. (France) **50**, 3175 (1989).